Proceedings of the Tenth Pacific Conference on Earthquake Engineering
Building an Earthquake-Resilient Pacific
6-8 November 2015, Sydney, Australia

Deformation Capacity of RC Structural Walls without Special Boundary Element Detailing

C.J. Motter[1] and J.W. Wallace[2]

[1]*The University of Auckland, Auckland, New Zealand*

[2]*The University of California, Los Angeles, United States of America*

ABSTRACT:

Despite the abundance of large-scale laboratory tests of RC structural walls, few tests have been conducted on walls with light-to-moderate amounts of boundary transverse reinforcement, thicker cross-sections, and modest axial load levels. Two large-scale walls with rectangular cross-sections, with differing amounts of boundary longitudinal reinforcement, and without ACI 318-11 Special Boundary Elements were tested under a constant axial gravity load of $0.053A_g f'_c$ with reversed-cyclic, quasi-static lateral loading and overturning moment applied at the top of the wall. The applied moment gradient was consistent with the lower 1.5-stories of a 10-story building. The primary objective of the study was to ascertain the deformation capacity (plastic hinge rotation capacity) of the walls. Minimal strength degradation was evident in both specimens tested through loading cycles that produced 1.0% plastic hinge rotations. Significant strength degradation and damage occurred during loading cycles to 1.5% plastic hinge rotation. Failure was characterized by crushing and spalling of cover concrete, followed by buckling of wall longitudinal reinforcement, and eventual bar fracture and core crushing.

1. INTRODUCTION

The use of structural walls to resist lateral loads from earthquakes and wind in reinforced concrete buildings is commonplace. Walls are typically designed to remain elastic for wind loads, but during earthquake shaking mid- and high-rise walls typically yield at the base at moderately low shear demands (e.g., $0.167\sqrt{f'_c}$ -MPa, $2\sqrt{f'_c}$ -ksi). Yielding is typically assumed to concentrate over a plastic hinge length, which extends upwards from the base of the wall (e.g., Paulay, 1986). In this modelling approach, post-yield lateral deformation (i.e., plastic drift) of the wall is linearly-dependent on the plastic hinge rotation, which is computed as the product of the plastic curvature and the plastic hinge length. In displacement-based design of walls, the design lateral deformations are used to determine the plastic hinge rotation, which is used to assess the need for boundary element detailing (Wallace and Moehle, 1992; Moehle, 1992; Wallace and Moehle, 1993). For mid-and high-rise walls, special boundary elements detailed in accordance with ACI 318-11 Section 21.9.6.4 are typically required at the lower stories, in order to provide lateral confinement of boundary element concrete and restrain buckling of longitudinal reinforcement. Above the plastic hinge region, where significant yielding is not expected, special boundary elements are not required and boundary transverse reinforcement is based on ACI 318-11 Section 21.9.6.5. In this study, two reinforced concrete structural walls without special boundary elements were tested to failure under constant axial load and quasi-static, reversed-cyclic loading (shear and moment). The primary objective of this study was to assess the performance of thick, flexure-controlled walls with modest axial loads and with boundary transverse reinforcement required by ACI 318-11 Section 21.9.6.5.

2. SPECIMEN DESIGN

In order to assess the performance of RC structural walls without special boundary elements, two specimens, referred to as W1 and W2, were designed and tested in the UCLA Structural Earthquake Engineering Laboratory. The test specimens were designed to be roughly one-half-scale based on an assumed prototype. The cross-sections for both walls were rectangular with an asymmetric layout of reinforcement (Figure 1). The primary test variables were the quantity of wall boundary longitudinal and transverse reinforcement, which led to variation in the s/d_b ratio, which is the ratio of the vertical spacing of boundary transverse reinforcement, s, to the bar diameter of the boundary longitudinal reinforcement, d_b. A larger s/d_b ratio indicates an increased likelihood for buckling of boundary longitudinal reinforcement. The s/d_b ratios at each end of the wall were 5.3 and 4.6 for W1 and 6.4 and 16.0 for W2. Therefore, the likelihood of bar buckling was significantly larger at one boundary of W2 relative to the other wall boundaries.

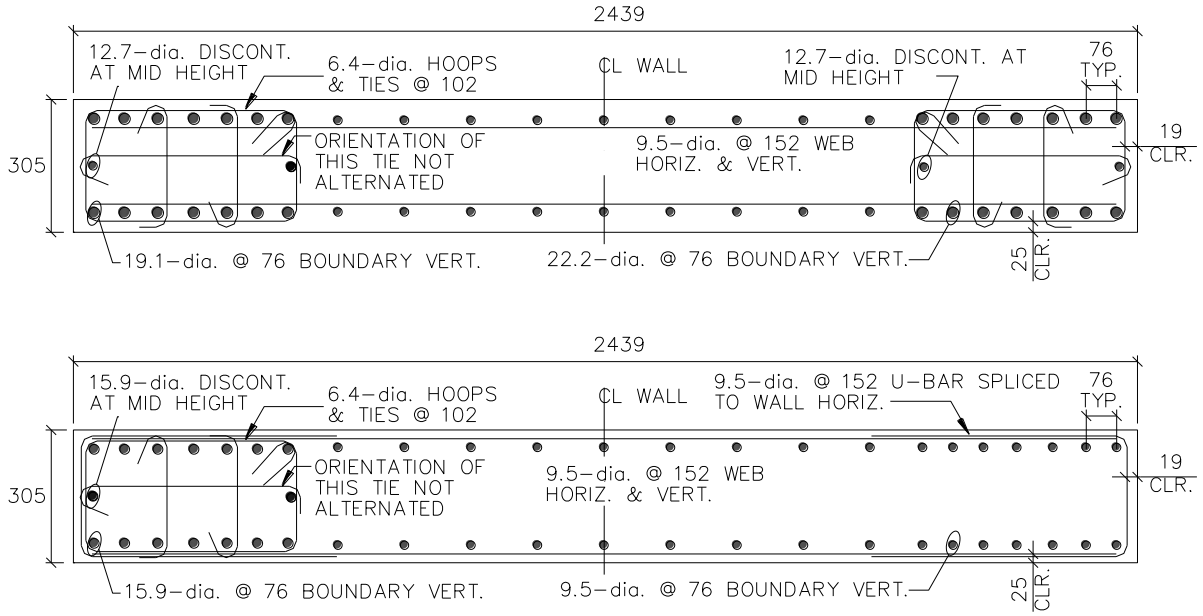

Figure 1. Shear Wall Cross-Sections (dimensions in millimetres) (top: W1, bottom: W2)

An intermediate level of wall boundary transverse reinforcement, which provides a lower level of confinement than an ACI 318-11 Section 21.9.6.4 special boundary element, is representative of a mid-to-upper-level story for a high-rise reinforced concrete building in a zone of moderate-to-high seismic risk. At both boundaries of W1 and at one boundary of W2, reinforcement was provided to satisfy provisions for an intermediate level of wall boundary transverse reinforcement (sometimes referred to as an Ordinary Boundary Element (OBE), as used in NIST GCR 11-917-11), namely ACI 318-11 Section 21.9.6.5(a), which requires 203-mm maximum vertical spacing of this reinforcement. Assuming 13-mm diameter hoops and ties at 203-mm spacing for the prototype led to 6.4-mm diameter hoops and ties at 102-mm spacing for the test specimens. W2, which has light boundary reinforcement at one boundary, is intended to be representative of the upper-level stories in a typical high-rise wall, where the boundary longitudinal reinforcement ratio is less than $400/f_y$ (which corresponds to ρ = 0.0067 for reinforcement with a specified yield strength of 60-ksi = 414-MPa, which is common is the United States). This led to the use of 14- 9.5-mm longitudinal bars at the W2 wall boundary (ρ = 0.0061) with minimum boundary transverse reinforcement. This minimum reinforcement consisted of 9.5-mm U-bars engaging wall boundary longitudinal reinforcement and spliced to the 9.5-mm web transverse reinforcement at both ends of the wall per ACI 318-11 Section 21.9.6.5(b). For W1, the horizontal web bars were embedded (without hooks) into the cores of the ordinary boundary elements. It is noted that for both W1 and W2, longitudinal and transverse wall web bars were selected to meet the code minimum reinforcement ratio, which is $\rho_l = \rho_t$ = 0.0025 per ACI 318-11 Section 21.9.2.1.

Each of the walls tested in this study were used previously for testing of steel reinforced concrete (SRC) coupling beams (Motter et al, 2014), which resulted in significant damage at the beam-to-wall connection. This damage was repaired prior to testing of the walls, with photos of the repaired walls shown in Figure 2. The repairs at this region included removal of the embedded steel beams for W2, removal of damaged concrete, grouting of damage regions, and the use of steel plates and post-tensioned threaded rods to provide confinement. Because the coupling beam centrelines were located 1676-mm above the base of the 2438-mm long walls, a successful repair was not expected to significantly impact the post-yield performance of the wall, as damage for the flexure-controlled walls was expected to concentrate over an assumed plastic hinge length of $l_w/2$=1219-mm, where l_w is the wall length, which is located below the bottom of the steel plates. Therefore, the repairs were not expected to improve the post-yield performance of the specimens. During prior testing of the coupling beams, wall moments within the plastic hinge region produced flexural cracking, but generally did not cause yielding of wall boundary longitudinal reinforcement.

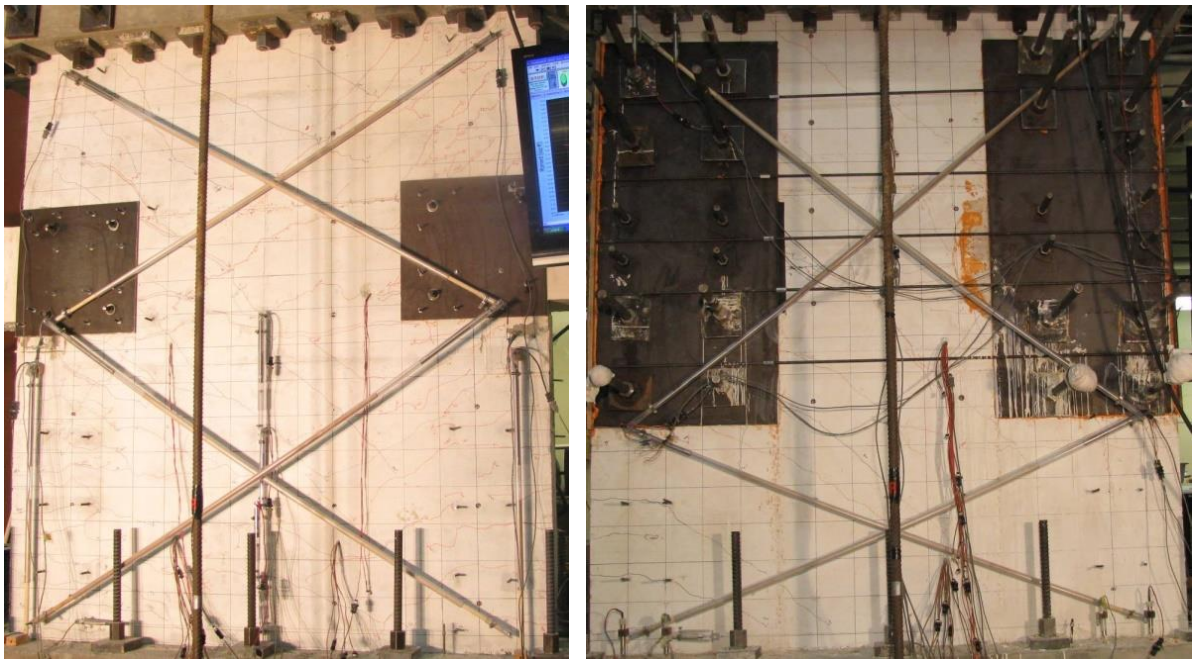

Figure 2. Photo of Repaired Walls Prior to Testing (Left to Right: W1, W2)

3. MATERIAL PROPERTIES

High-strength (~69.0-MPa = 10-ksi) hydro-stone grout was used to repair wall damage that occurred during coupling beam testing (Motter et al, 2014). Note that, because the wall yield moment was reached at relatively low shear stress (< $0.167\sqrt{f_c'}$ -MPa, $2\sqrt{f_c'}$ -ksi), concrete strength was not expected to significantly influence the wall capacity. Each test specimen included a construction joint that was located 1905-mm above the base of the wall, i.e., at the top of the coupling beams that were tested by Motter et al (2014). Based on average values from tests on 152-mm x 305-mm concrete cylinders, the tested concrete strength, $f'_{c,test}$, for the f'_c = 31.0-MPa mix was 50.1-MPa and 47.7-MPa for concrete below and above the construction joint, respectively, for W1 and 40.7-MPa and 39.7-MPa for concrete below and above the construction joint, respectively, for W2.

The tested yield stress ($f_{y,test}$), ultimate stress ($f_{u,test}$) and % elongation (% elong.) for all reinforcement used in the test specimens is provided in Table 1. All reinforcement 9.5-mm in diameter or larger was U.S. Grade 60 (specified yield stress of 60-ksi = 414-MPa), with the values in Table 1 coming from the provided mill certificates. The wall boundary transverse reinforcement consisted of 6.4-mm diameter U.S. Grade A36 undeformed bars (minimum specified yield stress of 36-ksi = 248-MPa), with the values in Table 1 taken as the average from three tensile tests.

Table 1. Reinforcement Properties

	W1					W2			Both
	#7	#6	#5	#4	#3	#5	#4	#3	#2
$f_{y,test}$ (MPa)	490	534	474	497	441	426	497	469	351
$f_{u,test}$ (MPa)	659	717	720	752	707	577	739	724	499
% elong.	19	14	15	13	14	19	15	14	21

4. TEST SET-UP AND TESTING PROTOCOL

Both specimens were tested at the University of California, Los Angeles Structural/Earthquake Engineering Testing Laboratory. Using the test set-up shown in Figure 3, the specimens were subjected to a constant axial (gravity) load of 1220-kN ($0.053A_g f'_c$) and quasi-static, reversed-cyclic lateral loading and overturning moment applied at the top of the wall. Two 1780-kN (max.) actuators with +/- 457-mm stroke were used to apply wall overturning moment. The wall lateral shear force (and additional moment) was applied by a 1335-kN (max.) actuator with +/- 305-mm stroke and was reacted by the reaction blocks, which were stacked, grouted at the interfaces, and post-tensioned to the laboratory strong-floor with 32-mm diameter high-strength post-tensioning rod. The "concrete top beam" refers to a thickened portion at the top of the shear wall (poured continuously with the upper wall), which was constructed to facilitate anchorage to the steel loading beam (positioned across the top of the specimen). The top beam and footing were post-tensioned to the steel loading beam and the laboratory strong floor, respectively. A steel brace (not shown) was attached to the steel loading beam to prevent out-of-plane displacement or torsion of the specimen during testing. Loading jacks at the top of the steel loading beam were used to apply axial compressive load to the top of the wall, with additional axial load applied by the two vertical actuators.

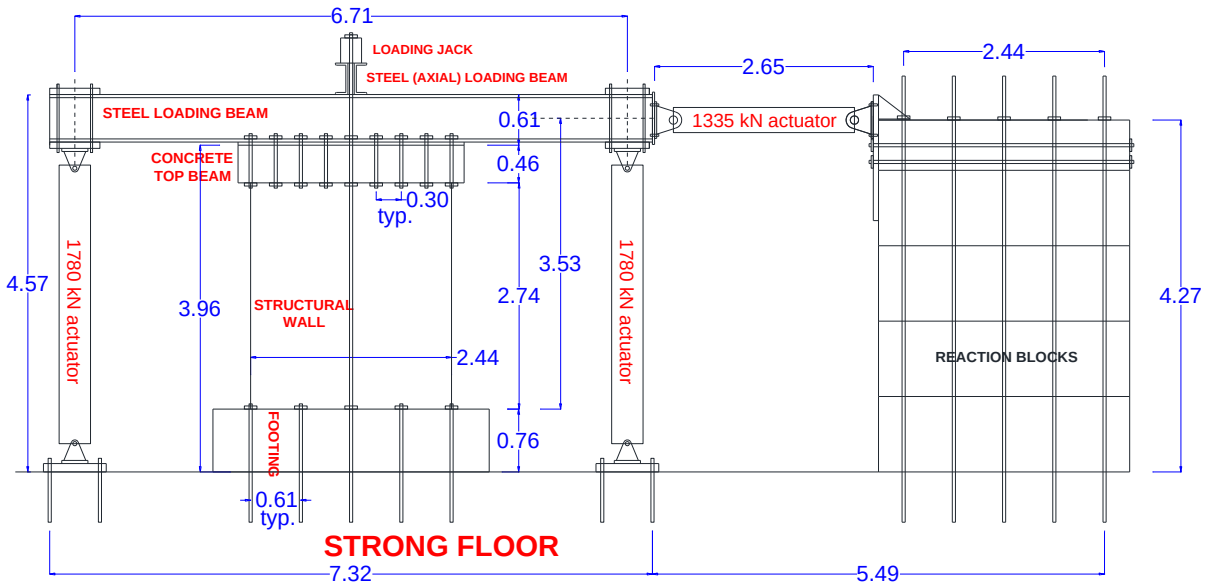

Figure 3. Test Set-Up (dimension in meters)

The applied moment gradient in the walls was constant and linear throughout testing, with the ratio of wall top moment to wall base moment held at 0.79. The selection of this ratio was determined by analysing an idealized 10-story structure with equal story heights and story masses using the equivalent lateral force procedure in accordance with ASCE 7-10 Section 12.8 (United States). In this approach, it was assumed that the test specimen walls, which were 2743-mm tall at approximately one-half-scale, represented the lowermost 1.5 stories of the 10-story structure. Using this approach, it was found that there was minimal variation in moment demand over the specimen height for a range of possible periods for the structure.

Both tests were displacement-controlled using the plastic hinge rotation measured by a pair of LVDTs, located near opposite ends of the wall, spanning from the footing to the assumed plastic hinge length. This length was taken as $l_w/2$=1219-mm for the first specimen but was taken to the base of the steel plates used for repair, which were located $3l_w/8$=914-mm above the base of the wall, for the second specimen, as the presence of the steel plates was expected to prevent the spread of plasticity into the repaired region. The loading protocols for both tests, shown in Figure 4, were identical between 0.125% and 1.5% rotation, with the exception of inadvertent loading from -0.25% rotation to -1.15% rotation (at a rate of roughly 0.07% rotation per second) during the first loading cycle at 0.25% rotation for W2. Relative to W1, additional low-level cycles were carried out for W2, as yielding was expected to occur at a smaller rotation due to the lower yield moment associated with the reduced quantity of wall boundary longitudinal reinforcement. Three cycles were carried out at all loading increments through 1.5% rotation. Beyond 1.5% rotation the testing protocol was based on the observed damage and response of the test specimens. For both specimens, failure initially occurred at one wall boundary. Asymmetric loading was then used in an effort to limit the level of compression applied to the boundary that had failed, thereby reducing the likelihood of fracture of the longitudinal bars at this side of the wall. This was done in an effort to generate failure at the other side of the specimen, noting that fractured bars would reduce the compression demand on the boundary that had not failed and reduce the likelihood that this failure could be achieved.

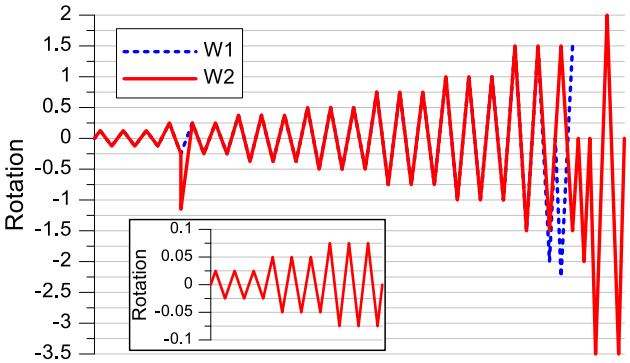

Figure 4. Loading Protocol

5. TEST RESULTS

For both walls, damage concentrated beneath the repaired region of the wall (Figure 5 and Figure 6) due to pre-existing damage, noting that the applied wall demands were largest at the base. For W1, damage concentrated at the wall boundary with a lower s/d_b ratio (i.e., at the side of the wall with 22-mm diameter longitudinal reinforcement), which was also likely the result of pre-existing damage, noting that this wall boundary was damaged more heavily during previous testing (Motter et al, 2014). For W2, damage concentrated at the wall boundary with a higher s/d_b ratio (i.e., with 9.5-mm diameter longitudinal reinforcement). With reference to the loading protocol shown in Figure 4, positive loading put the damaged wall boundary into compression for both W1 and W2.

For W1, no significant damage was observed through loading cycles at 1.0% rotation (Figure 5a). Spalling of cover concrete occurred during the first loading cycle at 1.5% rotation (Figure 5b). Increased spalling of cover concrete accompanied by buckling of longitudinal boundary reinforcement and some crushing of core concrete occurred during subsequent loading to 1.5% rotation in the positive loading direction and 2.0% and 2.25% in the negative loading direction (Figure 5c). The test was stopped after subsequent loading to 1.5% rotation in the positive direction (3rd cycle), which led to significant bar buckling and spalling and continued crushing of some core concrete (Figure 5d).

For W2, no significant damage was observed through loading cycles at 1.0% rotation, and the onset of spalling of concrete cover was observed after the first loading cycle at 1.5% rotation (Figure 6a). After the completion of all loading cycles at 1.5% rotation, more extensive spalling of cover concrete associated with the onset of buckling of longitudinal boundary reinforcement was observed (Figure 6b). More extensive spalling of cover concrete accompanied by bar buckling and some minor

crushing of core concrete is evident after completion of the one-half loading cycle to 2.0% in the negative direction (Figure 6c). After a large excursion to 3.5% rotation in the negative direction followed by loading in the positive direction to 2.0% rotation, extensive propagation of spalling and bar buckling is evident in addition to crushing of the concrete core (Figure 6d). The test was stopped after a second excursion to 3.5% rotation in the negative direction.

Figure 5. Damage photos for W1 after completion of cycle at (left to right): 1.0% rotation, 3rd cycle; 1.5% rotation, 1st cycle; -2.25% rotation (negative one-half cycle); 1.5% rotation, 3rd cycle (positive one-half cycle)

Figure 6. Damage photos for W2 after completion of cycle at (left to right): 1.5% rotation, 1st cycle; 1.5% rotation, 3rd cycle; -2.0% rotation (negative one-half cycle); +2.0% rotation (positive one-half cycle)

Assessment of the behaviour in the repaired (i.e., upper) portions of the walls could be carried out, but is likely unrepresentative of typical wall behaviour due to the significant alteration of the wall section properties associated with the steel plate and post-tensioning system used to makes the repairs prior to testing. Therefore, assessment of load-deformation response will focus on the non-repaired portion of the walls, i.e., the assumed plastic hinge region.

Minimal pinching and strength degradation in the load-deformation response (Figure 7) was evident for W1, until failure occurred during the third loading cycle at 1.5% plastic hinge rotation. In this paper, failure is defined to have occurred when the load at the peak of a cycle initially drops below 80% of the peak load and does not return to this value. Noting that the performance of an undamaged wall may have exceeded that observed in this test, failure occurred in the positive loading direction at a plastic (i.e., post-yield) rotation of roughly three times the yield rotation (noting that the reported plastic hinge rotation in Figure 7 is the sum of plastic and elastic rotation). In the negative loading direction, no significant strength loss was observed up to a plastic rotation of roughly six times the yield rotation.

Similar to W1, minimal pinching and strength degradation was evident in the load-deformation response for W2 (Figure 7) prior to failure (neglecting strength degradation relative to the peak strength observed during inadvertent loading to -1.15% rotation). Failure occurred at roughly 1.25% plastic hinge rotation during the first loading cycle to 2.0% rotation (after completion of three cycles at 1.5% rotation). For W2, which had an intermediate level of boundary transverse reinforcement (ACI 318-11 Section 21.9.6.5(a)) at one end and a minimum level of boundary transverse reinforcement (ACI 318-11 Section 21.9.6.5(b)) at the other end, failure occurred at the wall boundary with minimum transverse reinforcement. W2 had a lower yield moment and yield rotation than W1, and for W2 a plastic rotation in excess of six times the yield rotation was reached prior to failure. Similar to W1, the ductility of a wall with no prior damage may exceed that observed for W2.

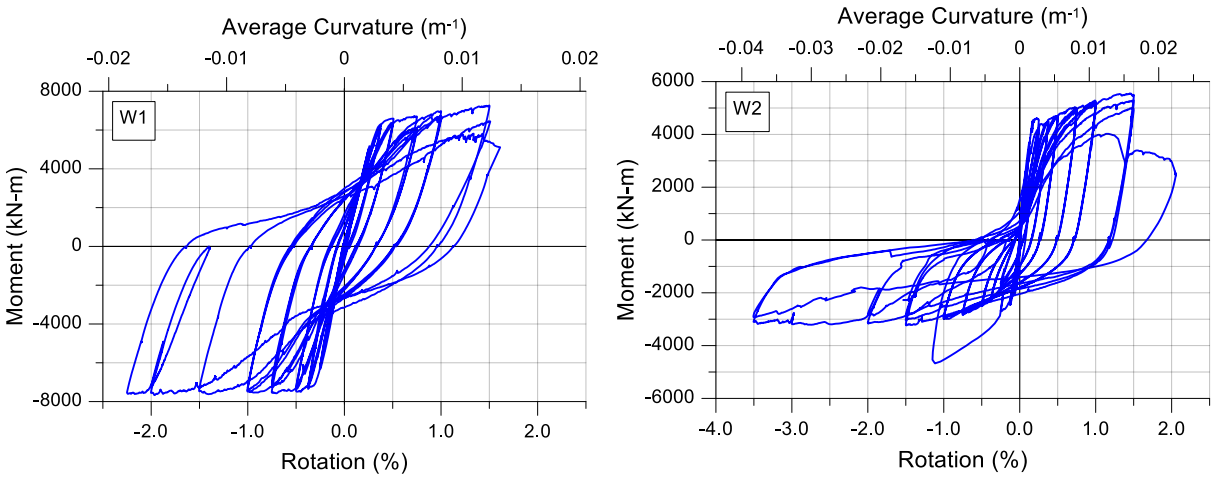

Figure 7. Load-Deformation Responses

Significant yielding is not expected in regions of walls with Ordinary Boundary Elements (ACI 21.9.6.5(a)) or minimum boundary transverse reinforcement (ACI 21.9.6.5(b)). To ensure "essentially elastic" behaviour, the PEER/ATC 72-1 (2010) report recommends that yielding in the upper levels of the wall be limited to tensile strains that do not exceed twice the yield strain or plastic rotations that do not exceed 1.2 times the yield rotation. The aforementioned plastic rotation capacity met or exceeded three times the yield rotation for both W1 and W2. These walls had applied axial loads of $0.032A_g f'_{c,test}$ and $0.040A_g f'_{c,test}$ (with $f'_{c,test}$ taken here as the tested compressive strength of concrete below the construction joint, with reference to Section 3), respectively, and length-to-thickness ratios of eight. Based on the test results, increasing the PEER/ATC 72-1 (2010) limiting tensile strains to four times the yield strain and the limiting plastic rotation to three times the yield rotation is suggested for walls with two layers of reinforcement, with axial load levels not in excess of $0.04A_g f'_c$, and with length-to-thickness ratios not in excess of eight. It is noted that thinner walls, or walls with larger axial loads, may fail at lower plastic rotation demands than the walls tested in this study.

6. SUMMARY AND CONCLUSIONS

In this study, two large-scale walls with rectangular cross-sections and asymmetric boundary longitudinal reinforcement were tested to failure under constant gravity loading and quasi-static, reversed-cyclic lateral (seismic) demands. These walls had light-to-moderate amounts of boundary transverse reinforcement and modest axial load levels, noting that there is a lack of test results for these conditions. The test specimens included repairs that were made at roughly mid-height due to damage obtained from use in previous coupling beam testing. The primary test variables were the amount of boundary longitudinal and transverse reinforcement, influencing the ratio of transverse reinforcement spacing to longitudinal bar diameter (s/d_b). The s/d_b ratio, which influences the likelihood of bar buckling, differed at each of the wall boundaries and ranged from 4.6 to 16.0. Neither of the test specimens included ACI 318-11 (Section 21.9.6.4) special boundary elements. The first test specimen had an intermediate level of boundary transverse reinforcement (in accordance with

ACI 318-11 21.9.6.5(a)), while the other specimen had an intermediate level of boundary transverse reinforcement at one end and minimum transverse reinforcement at the other end (in accordance with ACI 318-11 21.9.6.5(b)).

The primary objective of this study was to determine the deformation capacity in the plastic hinge region of the walls, located beneath the repaired regions. To accomplish this objective, these walls were tested under constant axial load ($0.053A_g f'_c$) with quasi-static, reversed-cyclic lateral loading and overturning moment applied at the top of the wall. The applied moment gradient was consistent with the lower 1.5-stories of a 10-story building, and the measured plastic hinge rotation was used to control the tests (displacement control). After completion of loading cycles that produced 1.0% plastic hinge rotations, minimal strength degradation was evident in both specimens. During subsequent loading cycles to 1.5% plastic hinge rotation, significant strength degradation and damage was observed. The failure sequence in these walls began with crushing and spalling of cover concrete and was followed by buckling of wall longitudinal reinforcement and eventual bar fracture and core crushing. For W1, failure occurred during the third loading cycle at 1.5% rotation, which corresponded to a plastic rotation of roughly three times the yield rotation. For W2, failure occurred during the first loading cycle to 2.0% rotation after the completion of three loading cycles at 1.5% rotation, which corresponded to a plastic rotation in excess of six times the yield rotation, noting that W2 had a lower yield moment and yield rotation than W1. Had the walls been tested in an undamaged state, the deformation capacity in the plastic hinge region would be expected to meet or exceed that of the walls tested in this study. In the upper regions of walls where significant yielding is not expected, the PEER/ATC 72-1 report (2010) recommends limiting the tensile strain demands to twice the yield strain or limiting the plastic rotation demands to 1.2 times the yield rotation. Based on the test results reported in this study, increasing the limiting tensile strains to four times the yield strain and the limiting plastic rotation to three times the yield rotation is suggested for walls with two layers of reinforcement, with axial load levels not in excess of $0.04A_g f'_c$, and with length-to-thickness ratios not in excess of eight.

REFERENCES

ACI Committee 318. (2011). Building Code Requirements for Structural Concrete (ACI 318-11) and Commentary, American Concrete Institute, Farmington Hills, MI.

ASCE. (2007). ASCE/SEI Standard 41-06, Seismic Rehabilitation of Existing Buildings. American Society of Civil Engineers, Reston, VA.

Moehle, J.P. (1992). Displacement-Based Design of RC Structures Subjected to Earthquakes. *Earthquake Spectra*, vol. 8, no. 3, pp. 403-428.

Moehle, J.P., Ghodsi, T., Hooper, J.D., Fields, D.C., and Gedhada, R. (2011). Seismic design of cast-in-place concrete special structural walls and coupling beams: A guide for practicing engineers. *NEHRP Seismic Design Technical Brief No. 6*, NIST GCR 11-917-11, Gaithersburg, MD.

Motter, C.J., Wallace, J.W., Fields, D.C., Hooper, J.D., and Klemencic, R. (2013). Large-Scale Testing of Steel Reinforced Concrete (SRC) Coupling Beams Embedded into Reinforced Concrete Shear Walls. *UCLA SGEL Research Report*, University of California, Los Angeles.

Paulay, T. (1986). The Design of Ductile Reinforced Concrete Structural Walls for Earthquake Resistance. *Earthquake Spectra*, vol. 2, no. 4, pp. 783-823.

PEER/ATC-72-1. (2010). Modeling and Acceptance Criteria for Seismic Design and Analysis of Tall Buildings. Pacific Earthquake Engineering Research Center (PEER) and Applied Technology Council (ATC) Joint Task Force.

Wallace, J.W., and Moehle, J.P. (1992). Ductility and Detailing Requirements of Bearing Wall Buildings. *Journal of Structural Engineering*, vol. 118, no. 6, pp. 1625-1644.

Wallace, J.W., and Moehle, J.P. (1993). An Evaluation of Ductility and Detailing Requirements of Bearing Wall Buildings using Data from the March 3, 1985, Chile Earthquake. *Earthquake Spectra*, vol. 9, no. 1, pp. 137-156.